DOI: 10.13009/EUCASS2022-4549

Restrike model for an MHD solver: application to plasma-assisted supersonic combustion in scramjet

Bourlet Aymeric, Labaune Julien*, Tholin Fabien*, Vincent-Randonnier Axel*, Pechereau François* and Laux Christophe ***
** ONERA, Office National d'Etudes et de Recherches Aerospatiales*
6 Chem. de la Vauve aux Granges, 91120 Palaiseau, France
***EM2C, CNRS*
CentraleSupélec, 3 rue Joliot Curie, 91190 Gif-Sur-Yvette, France

Abstract
Plasma-assisted combustion is a promising way to enhance the stability and ignition of combustion in scramjets. However, it is still challenging from a numerical standpoint due to the difficulties of coupling plasma, hydrodynamics, and combustion physics. For the studies of gliding arcs produced in a supersonic flow, we use a magnetohydrodynamical approach to simulate the arc in the flow with very reasonable time and space steps. With that approach, we were able to reproduce the dynamics of discharges in supersonic non-reactive flows at the scale of the LAERTE combustor in ONERA.

1. Introduction

DC arcs discharges are a promising way to enhance and stabilize combustion in scramjets. These devices may use plasma in critical phases of the flight when they are not in standard operating conditions, such as the acceleration phase toward hypersonic flight [1]. However, as many issues and uncertainties still exist, plasma-assisted combustion technology is unavailable. Most research for developing plasma-assisted combustion for propulsion is experimental, and it explores a large variety of discharges and geometries [2]. Limited research with numerical tools in a complete chamber was produced due to the difficulty of creating a model able to handle both plasma and combustion physics in a realistic timescale. Numerical approaches use approximations due to the computational cost required for the plasma simulation, as the discharge dynamics need shorter time and space steps than combustion in most cases. The classical approach to combustion in supersonic flows considers the plasma as a fixed volumetric power source [3], which is reliable for discharges such as nanosecond repetitive discharges that stay at a fixed location in the fluid [4]. When DC arcs are used, however, the plasma is transported by the flow. A fixed deposition of power in the fluid cannot accurately describe the plasma-flow interaction, in particular the amount of energy deposited by the plasma into the gas, the temperature reached by the gas, and the location of energy deposition in the chamber.

To simulate such arcs, our approach is to solve the plasma physics with a classical magneto-hydrodynamic model (MHD) [5]. The model assumes the quasi-neutrality of the arc. Hence, there are no space charges in the system. This approach allows larger space and time steps in comparison of multi-fluid plasma simulation because it allows cells to be much larger than the Debye length. To alleviate the constraints of the quasi-neutral approximation, the MHD model has been augmented in this work with a simplified macroscopic model for streamer discharges to deal with arc restrike phenomena.

The first part of this paper briefly describes the model and its numerical implementation. In the second part, we present a series of simulations aiming to reproduce the physics of the discharges observed in experiments in the supersonic combustor LAERTE in ONERA. We introduce the experimental setup that serves as our simulation's basis, then we explicit the inputs of the simulations for the two studied cases. To finish, we show the simulation results and provide an analysis of the discharge dynamics in the supersonic flow.

2. Model description

2.1 Model description

The model of plasma-assisted combustion simulation should be able to reproduce accurately the physics of the hydrodynamics, the combustion, and the plasma. We choose to solve the Navier-Stokes equations to retrieve the dynamics of compressible supersonic flows. We add source terms in the system of equations to account for different

DOI: 10.13009/EUCASS2022-4549

plasma effects: species production rates dependent on the electric field, Laplace force, and Joule heating.. Because the DC arc current is of the order of 1 A, the magnetic fields are too low to generate significant Laplace forces. Furthermore, we have not yet considered plasma chemistry containing free electron and ions. Then in the following, we only account for the Joule heating

The model mathematically translates into the Navier-Stokes equations as described in [6]:

$$\frac{\partial}{\partial t}\left(\bar{\rho}\tilde{Y}_\alpha\right) + \frac{\partial}{\partial x_j}\left(\bar{\rho}\tilde{u}_j\tilde{Y}_\alpha\right) = \frac{\partial}{\partial x_j}\left(-\overline{\rho u_j'' Y_\alpha''} - \bar{J}_j^{Y_\alpha}\right) + \bar{\dot{\omega}}_\alpha \tag{1}$$

$$\frac{\partial}{\partial t}\left(\bar{\rho}\tilde{u}_i\right) + \frac{\partial}{\partial x_j}\left(\bar{\rho}\tilde{u}_j\tilde{u}_i\right) = \frac{\partial}{\partial x_j}\left(-\overline{\rho u_j'' u_i''} - \bar{P}\delta_{ij} + \bar{\tau}_{ij}\right) \tag{2}$$

$$\frac{\partial}{\partial t}\left(\bar{\rho}\tilde{e}_t\right) + \frac{\partial}{\partial x_j}\left(\bar{\rho}\tilde{u}_j\tilde{e}_t\right) = \frac{\partial}{\partial x_j}\left(-\overline{\rho u_j'' e_t''} - \bar{J}_j^{e_t} + \tilde{\sigma}_{ij}\tilde{u}_i\right) + \omega_{Joule} \tag{3}$$

By convention, for a quantity φ, the notation $\overline{\varphi}$ is the Reynold averaging of φ; $\widetilde{\varphi}$ is a mass-weighted Favre averaging defined by $\widetilde{\varphi} = \overline{\rho\varphi}/\bar{\rho}$ and φ'' is the associated fluctuation defined by $\varphi'' = \varphi - \widetilde{\varphi}$.
In the mass balance equation (1), ρ is the density; Y_α is the mass fraction of species α; u_j is the j-component of the fluid velocity vector u; $J_j^{Y_\alpha}$ is the j-component of the molecular diffusion flux for the chemical species α; $\dot{\omega}_\alpha$ is the production rate of species α if positive or the consumption rate if negative. In the momentum balance equation (2), P denotes the pressure tensor and τ_{ij} is the viscous stress tensor term. In the energy conservation equation (3), e_t is the total energy per unit of mass and $J_j^{e_t}$ is the j-component of the total energy molecular flux. The term ω_{Joule} denotes the volumetric heating in the fluid by the Joule effect.

This work assumes the fluid is air in local thermodynamic equilibrium. The thermodynamic and transport properties of air are taken from the work of d'Angola [7], which gives analytical fits of the properties of equilibrium air at temperatures ranging from 50 to 60 000 K and pressures ranging from 0.01 to 100 atm. This work used these expressions to tabulate the enthalpy, heat capacity, entropy, electric and thermal conductivities, viscosity, and mean molar mass. We interpolate these data on the temperature and pressure during the computation when needed.

To compute the term ω_{Joule}, we use the relation (4) :

$$\omega_{Joule} = \frac{\mathbf{J}_\mathrm{q} \cdot \mathbf{J}_\mathrm{q}}{\sigma_q} \tag{4}$$

where $\mathbf{J}_\mathrm{q}$ is the electric current density and σ_q is the electric conductivity. The electric conductivity σ_q is obtained from the tabulated data, whereas $\mathbf{J}_\mathrm{q}$ is obtained using relation (5):

$$\mathbf{J}_\mathrm{q} = \sigma_q \boldsymbol{\nabla}\, \phi \tag{5}$$

ϕ is the electric potential, obtained by solving the conservation of electrical current (6):

$$\boldsymbol{\nabla} \cdot \left(\sigma_q \boldsymbol{\nabla}\, \phi\right) = 0 \tag{6}$$

The Navier-Stokes equations are solved with the CFD software CEDRE [8], while the plasma-related terms such as ω_{Joule} are computed in TARANIS, a quasi-neutral node-centered plasma solver in development at ONERA using the PETSsc library [9]. The choice of a coupling strategy is based on the versatility of this approach. Indeed, for hydrodynamics and combustion simulations, we need a solver that can handle complex reaction mechanisms, turbulence models, and wall models and incorporates a set of solvers for CFD. For the plasma part, the code must solve the current conservation equation, which is an elliptic problem requiring a different solver. In addition, the code must handle complex data structures. In our coupling strategy, we use two codes that take into account all the previous considerations.

The two codes exchange data at each iteration: CEDRE sends to TARANIS the fluid velocity, the temperature, the pressure, and the mass fractions of the species. TARANIS then returns the plasma source terms to CEDRE each iteration by using the CWIPI library [8]. The coupling scheme between the two codes is summarized in Figure 1.

DOI: 10.13009/EUCASS2022-4549

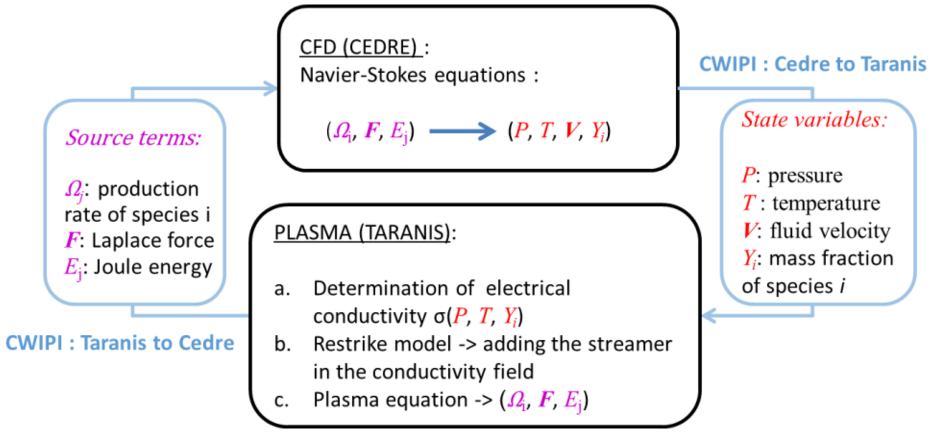

Figure 1: Coupling methodology used in this work

2.2 Restrike model

One crucial phenomenon appearing in the development of gliding arcs is the restrike of the discharges when the arcs reach a specific length. This breakdown event leads to the appearance of a new arc channel between the two arc branches, as shown in Figure 2.c. When a flow convects an arc, its electric resistance rises due to the stretching of the plasma channel. Consequently, the generator must deliver a higher voltage to the electrodes to sustain a constant current in the arc. Meanwhile, the gap between the two feet of the plasma stays roughly the same because each foot remains attached to the electrodes.
Hence, the electric field between the two arc branches increases until it reaches the breakdown electric field, which may form a streamer discharge. The streamer connects the arc branches or the electrodes, and its channel offers a new path to the electrical current. If the electrical current is high enough, the channel heats up until it becomes a new arc channel, which shortcuts the old arc and eventually leads to the extinction of the old channel.

Table 1: Input parameters of the restrike model

Phase of the streamer evolution	Input parameters	Values
Streamer initiation	Breakdown reduced field	125 Td
Streamer propagation	Conductivity threshold	1 S/m
Streamer-arc transition	Channel conductivity	1 S/m
	Channel radius	150 µm
	The time limit for the arc transition (Decay time)	1 µs

This restrike is the primary mechanism limiting the length of the arc discharge and controls the location where the energy is deposited in the chamber. However, a quasi-neutral solver cannot simulate this phenomenon because it relies on the formation and propagation of highly non-equilibrium and non-neutral streamer discharges. To address this issue in our simulation, we use a specific model of restrike presented in previous work [10], and Table 1 shows its input parameters. First, it checks whether the maximum reduced electric field is greater than the breakdown field. In this case, a streamer is artificially created. We assume that the streamer follows the direction of the electric field, so we compute the electric field line from the highest reduced electric field cell to a sufficiently high conductivity cell, which may be inside an arc branch or an electrode.

DOI: 10.13009/EUCASS2022-4549

Next, the restrike model adds a low conductivity channel along the electric field line corresponding to the streamer channel; its radius and conductivity value are fixed input parameters set to r = 150 µm and σ = 1 S/m. The code sustains and convects the low conductivity channel through the iterations, letting the electric current obtained by TARANIS heat the modeled streamer to an arc temperature. The electric current in the plasma channel depends on the relative resistance of the streamer compared with the arc one. Hence, it may be heated to an arc temperature or not. In the latter case, we disable the streamer after a particular duration. This duration is related to the characteristic time of streamer decay, namely 1 µs.

3. Simulations setup

3.1 Introduction of the experimental cases

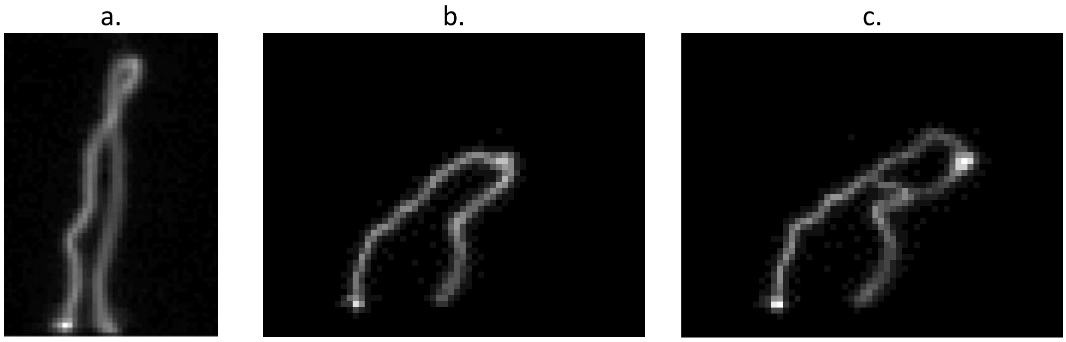

Figure 2: High-speed camera shots of the arc produced at the injector. a) no crossflow in the chamber; b) arc convected by crossflow; c) restrike of the discharge. The scales of image a) and images b) and c) are different.

The objective of this work is to reproduce the discharges observed in prior experiments at the LAERTE facility at ONERA [11]. The LAERTE facility is a supersonic combustor, working at Mach 2, dedicated to studying ignition conditions of reactive mixtures in supersonic flows. Because the combustor walls are not cooled, it operates with short bursts of combustion. Typically, in the experiments described here, combustion of H_2 occurs for approximately 10 s, whereas the plasma discharge is generated for about 2 s.

A special electrode system is built in a gas injector, as shown in the mesh in Figure 4. The two electrodes are assembled in a coaxial way: the anode is at the center of the electrode, it has a 2 mm-wide needle shape; the cathode is the injector's body surrounding the anode. In this system, the injected fluid flows into the cylindrical gap separating the two electrodes. The anode is connected to the high voltage port of the power supply while the cathode is grounded.

We reproduced two experimental cases in this work:

- Discharge alone. In this first case, the air in the chamber is at rest, at a temperature of 300 K and a pressure of 1 bar. The injector supplies air into the chamber at a flow rate of 7.14 g/s, at 300 K, 4.61 bar. The air coming from the outlet of the injector is supersonic. The power supply delivers a constant current of 1 A to the plasma generation module in these flow conditions to produce an arc at the top of the injector.

- Discharge in crossflow. In this second case, the plasma and the injection properties are identical to case 1. The difference is the presence of an air crossflow in the chamber of the LAERTE with a Mach number M=2, a static temperature T_i = 1540 K and a static pressure Pi = 4.1 bar at rest. These conditions correspond to a fluid velocity of 1180 m/s at 950 K and around 0.55 bar.

Figure 2 shows experimental shots of the plasma taken with a high-speed camera, with the image (a) showing the arc without crossflow and image (b) with crossflow. For reference, in both photos, the arc roots are separated by a distance of approximatively 2 mm. When the air in the chamber is at rest, the arc extends vertically over distances of 1 to 2.5 cm, following a statistic due to the restrike events. When there is a crossflow, the arc is much shorter, typically extending to a height of 5 mm, and it tends to develop more horizontally. In the crossflow, the standard deviation of the arc length is smaller. This could indicate that the development of the arc in the crossflow is more constrained, making its trajectory more predictable.

DOI: 10.13009/EUCASS2022-4549

3.2 Meshes

The 3D mesh used for the simulations is based on the geometry of the LAERTE, as shown in Figure 3. It contains 13.25 million cells. The mesh does not include the pre-heater nor the exhaust of the supersonic combustor. The inlet is at x = −0.4 m; the outlet at x = 0.45 m. At the inlet, we inject low-velocity air at the static temperature T = 1540 K and pressure P = 4.1 bar. The air flow is accelerated to Mach 2 after going through the Laval nozzle at x = −0.2 m. The plasma injector used in the experiment is located at x = 0 m; in this region, the smallest cells are 80 µm tetrahedra. The height of the chamber in the injector region is 3.54 cm with a constant width of 2 cm.

We compute plasma properties only in a smaller subdomain to reduce the computational load because the arc is located in a small volume at the top of the injector. The subdomain mesh presented in Figure 4 includes the volume of the injector and a 2-cm cube of fluid volume directly above the injector. It contains a total of 9.72 million cells. The boundary layer does not extend on the electrodes.

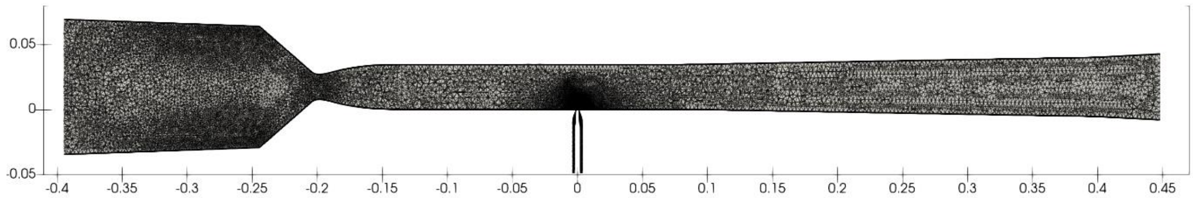

Figure 3: Mesh of the chamber used in CEDRE when crossflow is on.

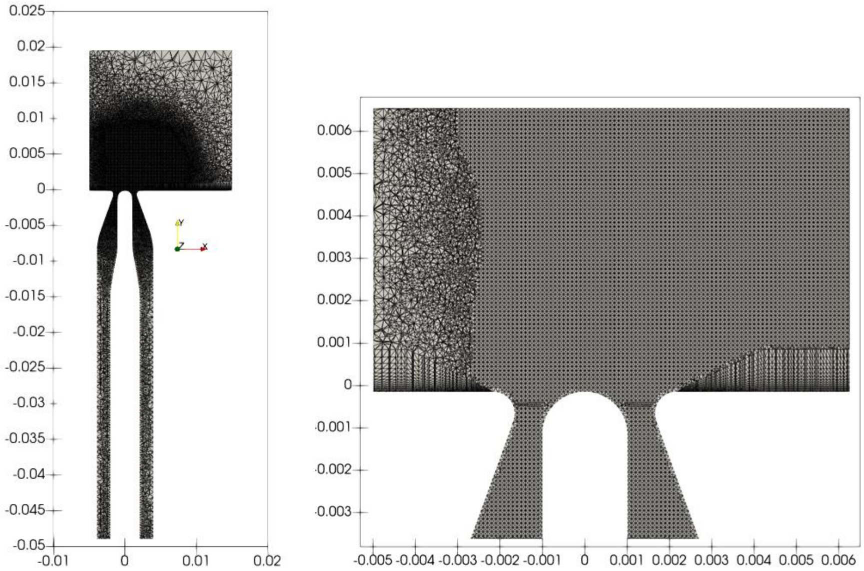

Figure 4: Mesh of the injector used in TARANIS.

4. Simulations results

4.1 First case: no crossflow

The temperature of all walls and electrodes is imposed at 300 K. The boundary conditions of the air volume above the injector correspond to the free stream conditions. The steady-state of the flow without plasma is computed and serves as the initial condition for the fluid state in the volume at the beginning of the simulation. Turbulence is treated with a k-ω RANS model in CEDRE. For the plasma, the electrical current is set to I = 1 A; the potential of the anode is

DOI: 10.13009/EUCASS2022-4549

dynamically adapted to match the current condition. A Neuman boundary condition is imposed at the wall inside the chamber for voltage computations, so the normal gradient of the electric field is null. This condition ensures that no electric current is lost in the wall of the supersonic duct, as it is a dielectric in the experiment. We produce an electric discharge in air at the injector for the first case. During the simulation, the discharge is convected by the flow, as shown in Figure 5.

The first breakdown occurs at t = 0 µs in the gap between the electrodes at $y = -1$ mm. During the first microsecond, the electric current heats the discharge to an arc temperature in the range of 6000 to 10 000 K. The temperature in the arc channel is not constant along the discharge length. This is because the flow properties and arc section vary significantly in the region where the arc is produced, and therefore the local cooling mechanisms vary along the length of the arc. During the next microseconds, the flow convects the discharge at the fluid velocity. The arc heats the surrounding air to temperatures ranging from 2000 to 4500 K, roughly 1 mm from the center of the arc.

A restrike phenomenon occurs between 24.7 µs and 25 µs, as shown by the new path taken by the electric current at 25 µs in Figure 5 (in purple). The restrike model has triggered this event. The arc continues its vertical development between 25 µs and 45 µs; there is no other restrike even if it becomes longer than the previous one at 45 µs. This is explained by an increase in the distance between the two arc branches due to the convection of the arc by the unsteady flow. We have no statistics yet on the restrike in these simulations. However, we observe a similar dynamic behavior in the experimental discharges shown in Figure 2a.

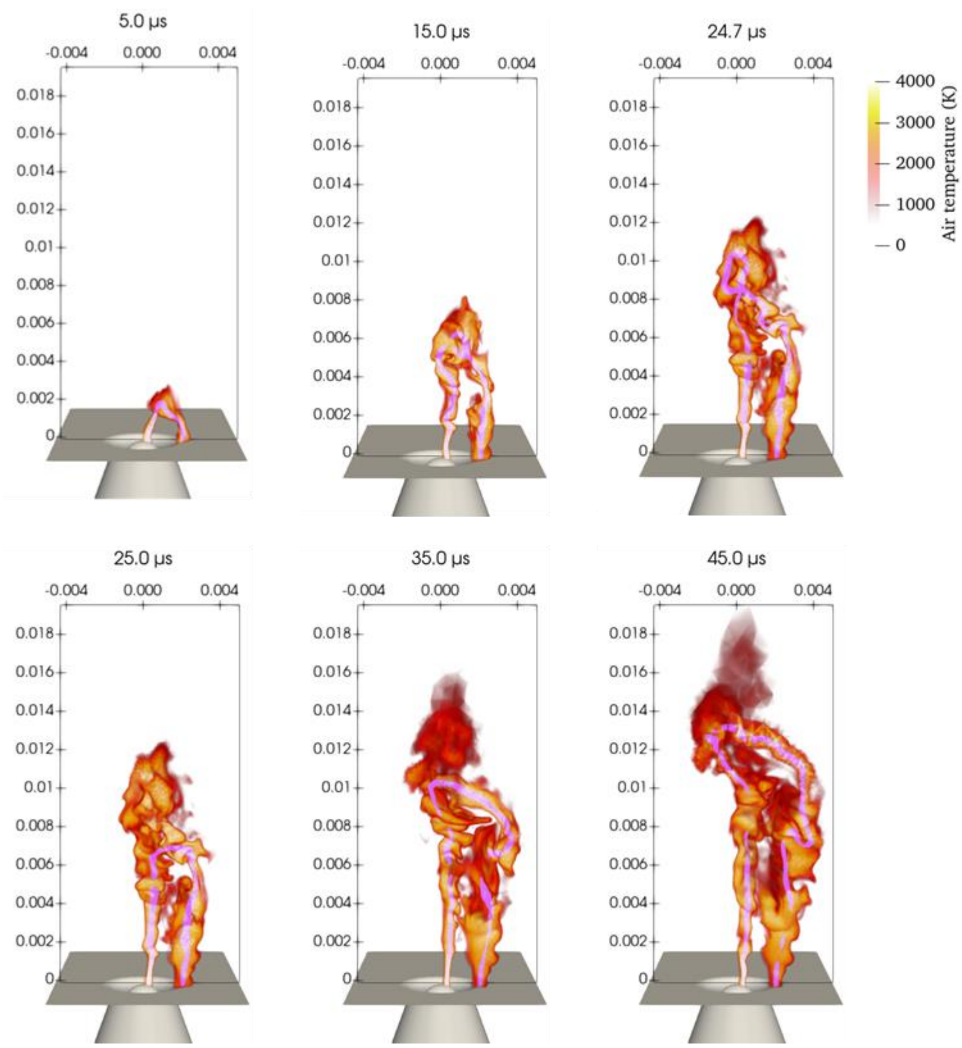

Figure 5: Sequence of the temperature field showing the discharge development at the injector. The purple path indicates the highest current density region.

DOI: 10.13009/EUCASS2022-4549

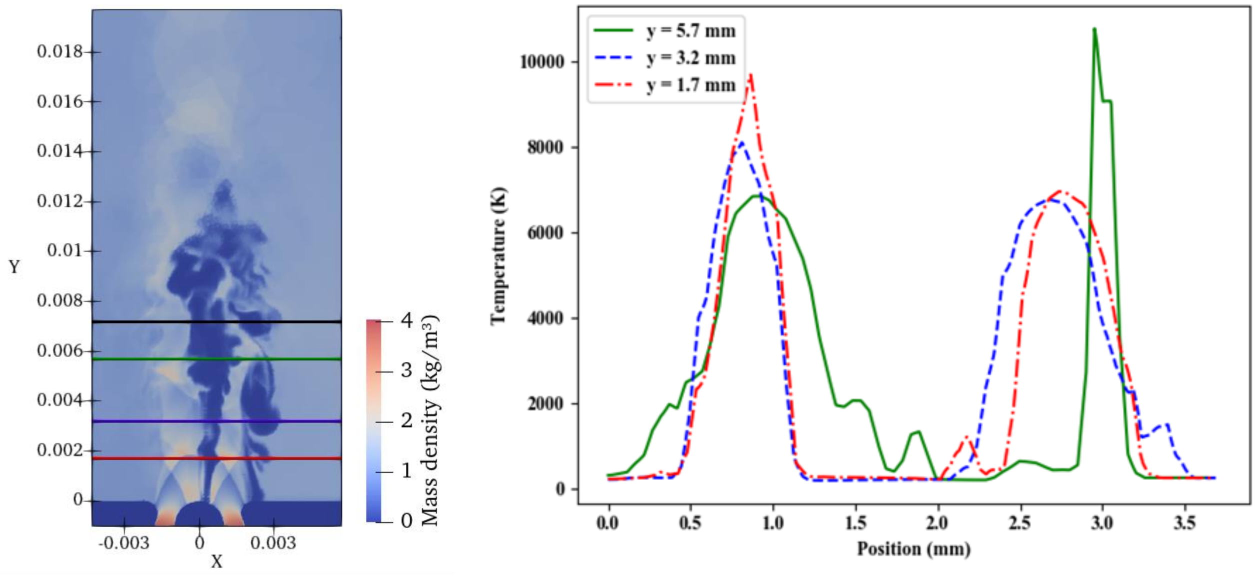

Figure 6: Left: mass density in the (x,y) plane. The black line corresponds to the maximum height of the arc at the selected instant, 25 µs. Red, blue, green lines correspond to the different y-positions chosen for the profile measurement. Right: temperatures profiles in the arc for different heights.

Next, focusing on the discharge at 25 µs just after the restrike, we show in Figure 6 the mass density profile on a slice going through the arc and different temperature profiles between the arc branches for different heights. The green, red and blue lines appearing in the slice indicate the different heights chosen for the profiles, though the profiles are not in the same plane displayed by the slice due to the 3D structure of the arc.

The mass-density field shows a complex flow. We observe a pattern of Mach disks at the top of the injector as the flow is supersonic when it leaves the injector. Due to the high temperature of the arc and its immediate surroundings, we observe a very low-density region. The low-density area is not directly a marker of where the plasma is, as it extends above the current position of the plasma's maximal y-position, marked by the black line in Figure 6. However, this low-density area outlines the regions heated by the plasma before the restrike and where reactive species for combustion might still exist.

In addition, the low-density regions play an essential part in the restrike phenomenon. Indeed, streamer breakdown occurs if the value of the reduced field E/N is above the breakdown field, where E is the magnitude of the electric field and N is the number densities of neutral particles. Because the mass density and the particle density are related, a streamer is most likely to start in the low mass-density region because E/N is higher.

The temperature profiles give information about the diameter of the arc. We see that the arc's radial temperature profile and radius are not uniform along the discharge length: the temperature ranges between 6000 and 10 000 K, whereas the radius ranges between 250 µm and 1 mm. As a rule of thumb, we see that the thinner the arc, the hotter it gets. This correlation between small arc radii and temperature seems reasonable given the following physical interpretation: Let us suppose all the electrical current I supplied by the generator goes through a cylinder electric arc of radius r. In this condition, the volumetric Joule heating in the arc is:

$$\omega_{Joule} = \frac{I^2}{\sigma_q \pi^2 r^4} \tag{7}$$

The temperature of an arc reaches an equilibrium temperature at which the Joule heating source equals the cooling fluxes (radiative, diffusive, convective). As seen in relation (7), if the arc radius is reduced due to hydrodynamical effects, the heating is more important and the equilibrium temperature becomes higher.

DOI: 10.13009/EUCASS2022-4549

4.2 Second case: simulation of the arc in a chamber with an M=2 air crossflow

For the second case in which the discharge propagates in an M=2 crossflow, the Navier-Stokes equations are solved in the chamber mesh shown in Figure 3. In contrast, the plasma source terms are only evaluated in the injector mesh. For combustion applications, the crossflow may consist of air and the injection of a mixture of air and fuel. To focus on the arc dynamics in this configuration, we considered as a first step in this study an injection of pure air

Figure 7 shows the discharge and flow temperature evolution. The plasma channel is seen at t = 0.5 µs at the top of the anode; then, the arc develops into the chamber during the following microseconds. The arc reaches a height of y = 5 mm during the first ten microseconds, and then it follows the jet stream in the x-direction up to x = 11 mm at 26 µs. At this point, the restrike model induces a streamer breakdown at x = 5 mm, occurring within 0.5 µs. After the first restrike, the old plasma channel remains a pocket of hot air convected by the flow. It cools down from 4500 K at 26.5 µs to 2000 K at 33 µs, likely thanks to the diffusion and mixing of the hot gas in the colder flow. For the combustion application, these hot gas bubbles should contain radicals produced by the arc. In Mach 2 flows, it may be possible that atomic species O and H will exist long enough in the gas at 2000 K to be convected over several centimeters and activate the combustion.

In Figure 8, we represent a sequence of the arc development during the first twelve microseconds. The darker region corresponds to the locations where the mass density gradient is important; it permits visualizing the shock structure at the top of the injector. In comparison with Figure 6, we retrieve shocks that look like Mach disks in the air jet, but they are deformed due to the M=2 crossflow coming from the negative x. Upstream of the jet between x = −10 mm and x = 0 mm, additional shocks are observed near the wall, where a recirculation zone appears.

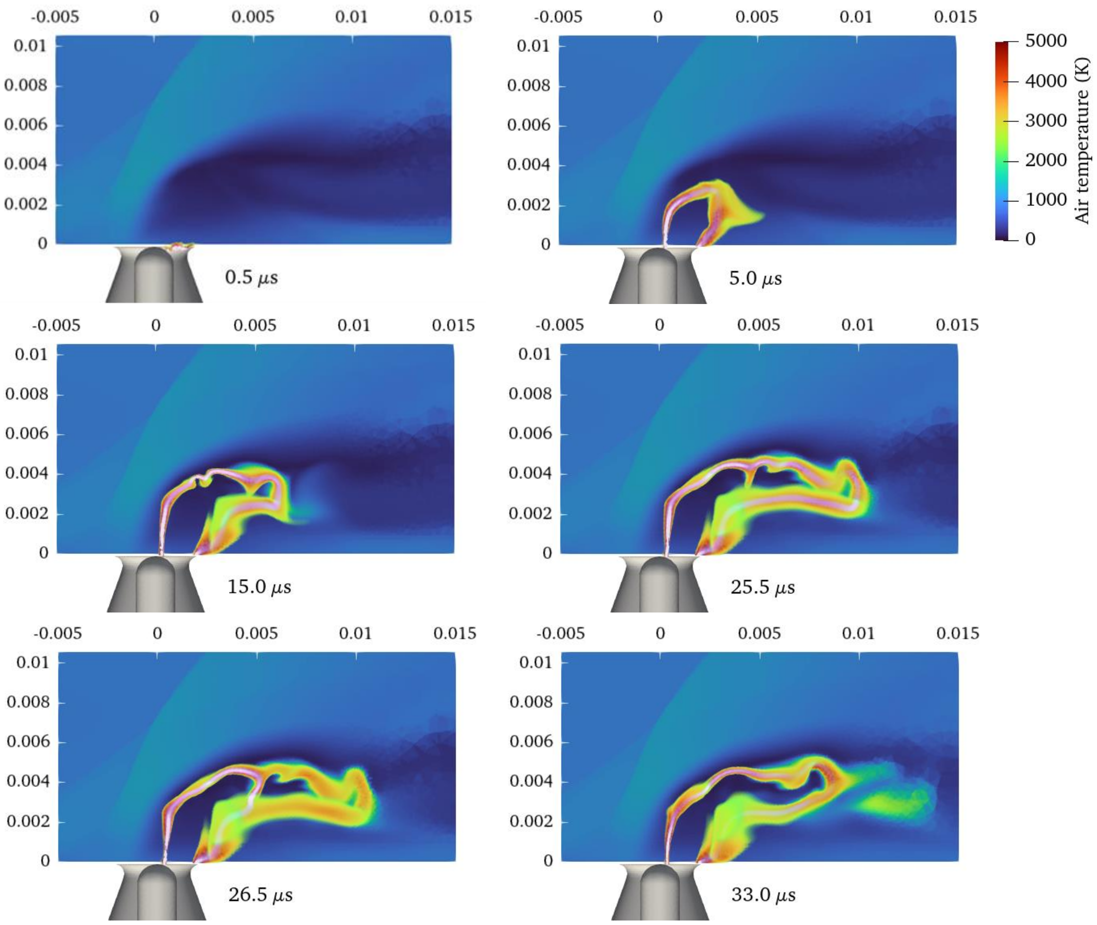

Figure 7: Sequence showing the discharge development in a crossflow at M=2 over the injector. The purple path corresponds to the highest electric current density.

DOI: 10.13009/EUCASS2022-4549

At the beginning of the simulation, we observe a shockwave coming from the arc formation and propagating at a supersonic velocity in the chamber. Such shockwaves are not produced in the subsequent restrikes; the first restrike is particular because there is no arc in the fluid when the breakdown occurs. This means that all of the 1-A current passes through a 150 µm-radius streamer channel with a conductivity of 1 $S.m^{-1,}$ which, according to Eqn. (7), gives a Joule heating in the streamer of $\omega_{\mathrm{Joule}} = 2.10^{14}\ \mathrm{W.m^{-3}}$. In comparison, when an arc already exists in the fluid, the streamer takes only a few percent of the total electrical current due to the difference between the electric resistance of the arc and the streamer, and Joule heating is of the order of $\omega_{\mathrm{Joule}} = 5.10^{12}\ \mathrm{W.m^{-3}}$. Consequently, the heating is much slower in case of a restrike, meaning that the pressure has more time for relaxing with its surrounding. Therefore, the first breakdown may be more difficult to simulate than the following restrikes.

During the first 7 µs, the arc extends in the y-direction until it reaches the shock at y = 4 mm. After 7 µs, the arc interacts with the shock and seems to change direction abruptly, following the shock structure as seen in Figure 8. We retrieve a result we observed experimentally, as seen on the left arc branch in Figure 2c. The arc follows the shock, which might be a mixing zone between the injected fluid with the crossflow. In the context of plasma-assisted combustion, the arc may interact in the region where fuel and oxygen are mixed; we may expect that it will speed up the kinetics in the mixing layer. In our simulation, the arc interacts with the recirculation zone downstream of the jet, which is another essential mixing zone in a combustion context. Still, the effects of that interaction remain unclear for the moment.

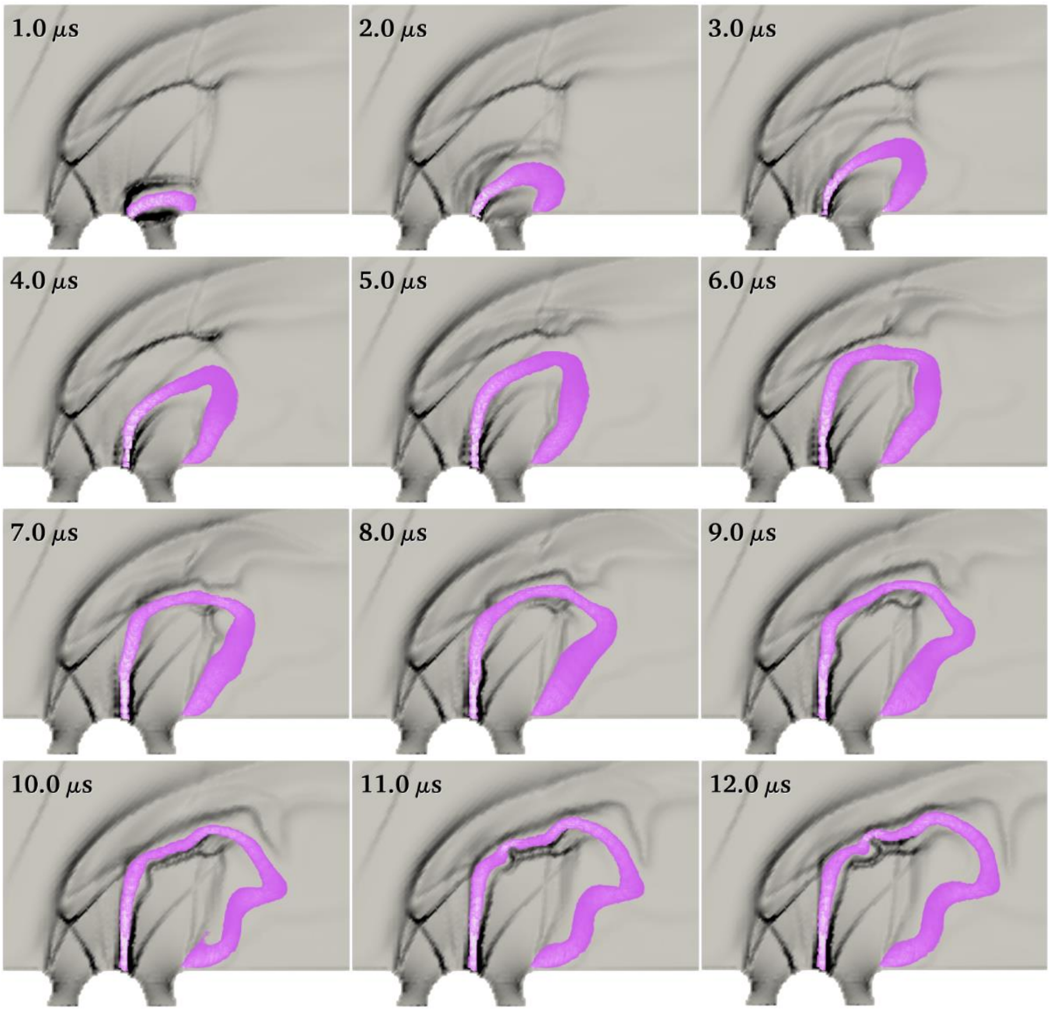

Figure 8: Sequence of pseudo-schlieren images in black, showing the gradient of mass density for shock visualization, while the discharge position (highest current density region) is indicated in purple.

DOI: 10.13009/EUCASS2022-4549

Conclusion

The numerical simulation of DC arcs in scramjets is a very challenging issue. This work has successfully taken advantage of a coupling strategy between the CFD code CEDRE, dedicated to combustion, and a quasi-neutral plasma code, TARANIS, augmented with a restrike model based on the physics of streamer discharges. Our first simulations in non-reactive flows display features observed in the experiments performed at the LAERTE facility. We retrieve the main characteristics of the dynamics of the discharges, more precisely the size, position, and restrike dynamics in terms of location and time. We showed that the plasma interacts with the shock structure, which impacts the shape of the arc in a way that matches the experimentally observed arc shape well.

This approach will be applied to PAC in future work, especially in supersonic combustion. As the dynamics of the DC arcs are properly computed without ad-hoc approximations concerning their presence, size, or location, this model is expected to be much more predictive than more straightforward approaches with fixed energy or active species depositions. Then, in forthcoming works, combustion kinetics will be added, and we expect a better probing and understanding of the detailed mechanisms of the plasma-enhanced combustion in scramjets with DC arcs. More precisely, the influence of the pseudo-periodical restrikes downstream is expected to be significant since the shortcut arc channels may be a source of hot and reactive recombining plasma pockets convected by the flow to well-mixed regions

Acknowledgments

Funding for this research has been provided by the French Defense Innovation Agency (AID) and ONERA through a Ph.D. grant.

References

[1] Jacobsen L. S. , Carter C. D. , Jackson T. A. , Williams S. , Barnett J. et al. 2008. Plasma-Assisted Ignition in Scramjets. *Journal of Propulsion and Power*. 24:641-654

[2] Leonov S. B. 2018. Electrically driven supersonic combustion. *Energies*. 11:1733

[3] Leonov S. B. and Yarantsev D. A. 2006. Plasma-induced ignition and plasma-assisted combustion in high-speed flow. *Plasma Sources Science and Technology*. 16:132

[4] Castela M. , Stepanyan S. , Fiorina B. , Coussement A. , Gicquel O. et al. 2017. A 3-D DNS and experimental study of the effect of the recirculating flow pattern inside a reactive kernel produced by nanosecond plasma discharges in a methane-air mixture. *Proceedings of the Combustion Institute*. 36:4095-4103

[5] Gleizes A. , Gonzalez J. J. , and Freton P. 2005. Thermal plasma modelling. *Journal of Physics D: Applied Physics*. 38:R153–R183

[6] Pelletier G. , Ferrier M. , Vincent-Randonnier A. , Sabelnikov V. , and Mura A. 2021. Wall roughness effects on combustion development in confined supersonic flow. *Journal of Propulsion and Power*. 37:151-166

[7] D'Angola A. , Colonna G. , Gorse C. , and Capitelli M. 2008. Thermodynamic and transport properties in equilibrium air plasmas in a wide pressure and temperature range. *The European Physical Journal D*. 46:129-150

[8] Refloch A. , Courbet B. , Murrone A. , Villedieu P. , Laurent C. et al. 2011. CEDRE Software. *Aerospace Lab*. 2:1-10

[9] Balay S. , Abhyankar S. , Adams M. F. , Brown J. , Brune P. et al. 2019. PETSc Users Manual. ANL-95/11 - Revision 3.11. Argonne National Laboratory.

[10] Bourlet A. , Labaune J. , Tholin F. , Vincent-Randonnier A. , Pechereau F. , and Laux C. O. 2022. Numerical model of restrikes in DC gliding arc discharges. In: *AIAA SCITECH 2022 Forum*. 0831

[11] Scherrer D. , Dessornes O. , Ferrier M. , Vincent-Randonnier A. , Moule Y. , and Sabelnikov V. 2016. Research on Supersonic Combustion. *Aerospacelab Journal*. 11:4